The Astrophysical Journal Letters, 843:L22 (5pp), 2017 July 10 https://doi.org/10.3847/2041-8213/aa79ef

Discovery of a Lensed Ultrabright Submillimeter Galaxy at $z = 2.0439$

A. Díaz-Sánchez[1], S. Iglesias-Groth[2,3], R. Rebolo[2,3,4], and H. Dannerbauer[2,3]
[1] Departamento Física Aplicada, Universidad Politécnica de Cartagena, Campus Muralla del Mar, E-30202 Cartagena, Murcia, Spain; Anastasio.Diaz@upct.es
[2] Instituto de Astrofísica de Canarias, Vía Láctea, E-38200 La Laguna, Spain
[3] Departamento de Astrofísica de la Universidad de La Laguna, Avda. Francisco Sánchez, E-38200 La Laguna, Spain
[4] Consejo Superior de Investigaciones Cientícas, E-28006 Madrid, Spain
Received 2017 June 9; revised 2017 June 14; accepted 2017 June 14; published 2017 July 7

Abstract

We report an ultrabright lensed submillimeter galaxy (SMG) at $z = 2.0439$, *WISE* J132934.18+224327.3, identified as a result of a full-sky cross-correlation of the *AllWISE* and *Planck* compact source catalogs aimed to search for bright analogs of the SMG SMM J2135, the Cosmic Eyelash. Inspection of archival SCUBA-2 observations of the candidates revealed a source with fluxes ($S_{850\mu m} = 130$ mJy) consistent with the *Planck* measurements. The centroid of the SCUBA-2 source coincides within 1 arcsec with the position of the *AllWISE* mid-IR source, and, remarkably, with an arc-shaped lensed galaxy in *HST* images at visible wavelengths. Low-resolution rest-frame UV-optical spectroscopy of this lensed galaxy obtained with 10.4 m GTC reveals the typical absorption lines of a starburst galaxy. Gemini-N near-IR spectroscopy provided a clear detection of H_α emission. The lensed source appears to be gravitationally magnified by a massive foreground galaxy cluster lens at $z = 0.44$; modeling with Lenstool indicates a lensing amplification factor of 11 ± 2. We determine an intrinsic rest-frame 8–1000 μm luminosity, L_{IR}, of $(1.3 \pm 0.1) \times 10^{13}\, L_\odot$, and a likely star formation rate (SFR) of $\sim$500–2000 $M_\odot$ yr^{-1}. The SED shows a remarkable similarity with the Cosmic Eyelash from optical-mid/IR to submillimeter/radio, albeit at higher fluxes.

Key words: galaxies: evolution – galaxies: high-redshift – galaxies: starburst – gravitational lensing: strong – infrared: galaxies – submillimeter: galaxies

1. Introduction

Submillimeter galaxies (SMGs) provide important clues on the formation and evolution of massive galaxies in the distant universe (Casey et al. 2014). These high-z dusty starbursts, peaking at redshift $z = 2.3$–2.5 (Chapman et al. 2005; Simpson et al. 2014; Strandet et al. 2016) are massive and most probably the progenitors of present-day ellipticals (e.g., Ivison et al. 2013). Given the typical sizes of starbursts (less than a few kiloparsecs; e.g., Hodge et al. 2016), even with ALMA and *HST* it is difficult to achieve the desirable spatial resolution to carry out detailed studies of star-forming regions in these dusty galaxies.

Strong gravitational lensing by massive galaxy clusters can enhance the apparent brightness of SMGs (Smail et al. 1997, 2002). Wide *Herschel* surveys such as H-ATLAS, HerMES, or the south Pole Telescope and the *Planck* space mission provided an increasing number of bright lensed SMGs (Negrello et al. 2010; Vieira et al. 2013; Weiß et al. 2013; Cañameras et al. 2015; Harrington et al. 2016; Strandet et al. 2016) that may allow their study at a resolution of 100 pc, close to the size of GMCs, and thus a better understanding of their ISM properties (see, e.g., Vlahakis et al. 2015; Swinbank et al. 2015) and a comparison of them with galaxies in the local universe. Among SMGs, the serendipitously discovered lensed galaxy SMM J2135-0102 at $z = 2.3259$ is outstanding (the Cosmic Eyelash Ivison et al. 2010; Swinbank et al. 2010; Danielson et al. 2011).

In this Letter, we present the first result of a search for the brightest examples in the sky of dusty star-forming high-redshift galaxies using data of the *Planck* and *WISE* space missions. We report the discovery of *WISE* J132934.18 +224327.3 as a magnified SMG at $z = 2.044$ with spectral energy distribution (SED) remarkably similar to that of the Cosmic Eyelash but higher apparent brightness at all wavelengths from visible to radio. We adopt a flat ΛCDM cosmology from Planck Collaboration XVI (2014) with $H_0 = 68$ km s^{-1} Mpc^{-1}, $\Omega_m = 0.31$, and $\Omega_\Lambda = 1 - \Omega_m$.

2. The Search

In order to find bright lensed SMGs in the full sky, we carried out a cross-matching between the *AllWISE*[5] and *Planck*[6] full-sky compact source catalogs. As a reference we adopted the SED of the Cosmic Eyelash (Swinbank et al. 2010), from the mid-infrared (MIR) to the submillimeter. Our aim was to identify candidates in these catalogs with MIR colors similar to the Cosmic Eyelash and strong submillimeter fluxes. First, we built a full-sky selection of galaxies verifying the color criteria $W1 - W2 > 0.8$, $W2 - W3 < 2.4$, $W3 - W4 > 3.5$ and detection at $S/N > 3$ in the four bands of the *AllWISE* catalog; we limited the sample to galactic latitude $b \geqslant 20°$. These color criteria were employed by Iglesias-Groth et al. (2017) in their near-infrared (NIR)/MIR search for lensed SMGs. These criteria also select SMGs with SEDs similar to the average SED of 73 spectroscopically identified SMGs from Michalowski et al. (2010), Hainline et al. (2011), and to the ALESS SMG composite SED (Swinbank et al. 2014). Only SMGs at $z = 2 - 2.8$ are expected to fulfill these color conditions.

Then, we requested the selected objects to have a *Planck* source detected within 5 arcmin with submillimeter flux ratios consistent with those expected for SMGs at $z = 2 - 3$. We found eight *WISE* candidates with SEDs consistent with the adopted references; however, the *Planck* submillimeter/millimeter maps for most of these sources clearly show

[5] http://wise2.ipac.caltech.edu/docs/release/allwise/
[6] http://pla.esac.esa.int/pla/#home

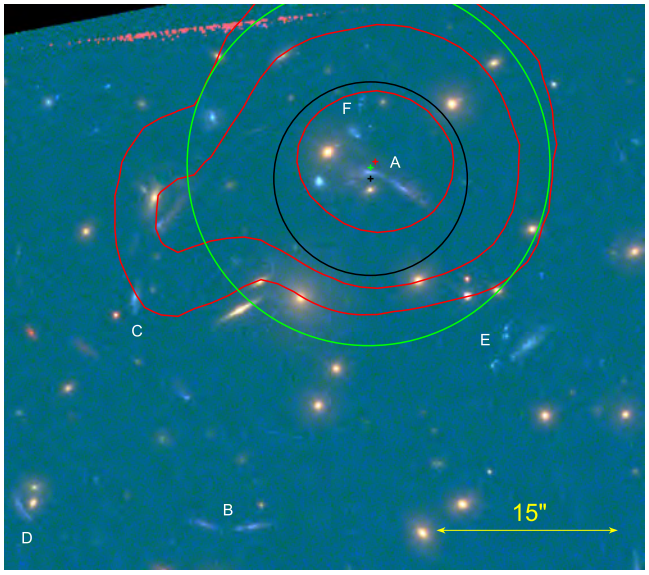

Figure 1. RGB image of the Cosmic Eyebrow with the *HST/WFC3* filters, blue F390W, green F606W, and red F160W. North is up; east is left. Red contours are *WISE* channel 4 and black (green) circles represent SCUBA-2 450 (850) μm detections. Crosses are the centroids of the *WISE* and SCUBA-2 detections, and they are within 1 arcsec from the *HST* main source of the arc. Capital letters indicate the six families of multiply lensed background galaxies used to perform a mass reconstruction of the foreground galaxy cluster (see the text).

contamination by galactic dust emission. Inspection of the *Planck* maps and available images from different optical and near-IR catalogs identified *WISE* J132934.18+224327.3 as the most likely counterpart of the submillimeter *Planck* source PCCS2 857 G007.94+80.29 and very promising candidate to an ultrabright SMG analog to the Cosmic Eyelash.

A subsequent search in CADC[7] provided detections by SCUBA-2 at James Clerk Maxwell Telescope of a submillimeter source with coordinates consistent within 1 arcsec with those of *WISE* J132934.18+224327.3, which could be responsible for the observed *Planck* submillimeter fluxes. In fact, the position of the source coincides with a strong lensing cluster SDSS 1329+2243 at $z = 0.44$ (Bayliss et al. 2014), which has been observed by Jones (2015) with JCMT/SCUBA-2 and reported a source in snapshot observations at 850 and 450 μm with fluxes $S_{450} \approx 605$ mJy and $S_{850} \approx 130$ mJy, consistent with being the main counterpart of the *Planck* source. Jones (2015) reported arc structures in Keck images suggesting it could be a lensed submillimeter source. Additional detections in the radio band are found in FIRST.[8]

We used Vizier at CDS[9] to find the most likely counterpart of the *WISE/Planck/SCUBA-2* source in the near-IR and visible. In *HST-ACS*[10] images, a lensed galaxy is also detected at less than 1 arcsec of *WISE* J132934.18+224327.3. We postulate that this lensed galaxy is the optical counterpart of the strong submillimeter and mid-IR source (see Figures 1 and 2(a)). Hereafter, we designate this lensed galaxy as the "Cosmic Eyebrow."

[7] http://www.cadc-ccda.hia-iha.nrc-cnrc.gc.ca/en/
[8] http://sundog.stsci.edu/first/catalogs.html
[9] http://vizier.u-strasbg.fr/viz-bin/VizieR
[10] http://archive.stsci.edu/

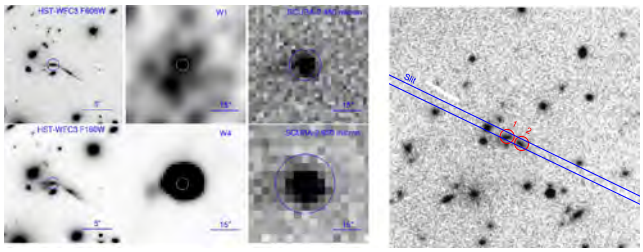

Figure 2. (a) Imaging of the Cosmic Eyebrow with *HST* (left column), *WISE* (middle column), and SCUBA-2 (right column). The circles represent the counterpart of the *Planck* source in the related imaging. North is up; east is left. (b) GTC g-band imaging of the Cosmic Eyebrow. We show the orientation of the long slit (slit width of 0.″8) for our spectroscopic observations. Spectra were extracted from the two encircled regions of the arc. North is up; east is left.

3. Observations and Data Reduction

3.1. GTC Spectroscopy

We have obtained spectroscopy of the lensed galaxy with the optical imager and spectrograph OSIRIS at the 10.4 m Gran Telescopio de Canarias (GTC), on the night of 2017 April 18 in clear conditions and dark moon with 0.″8 seeing. Observations were made using the low-resolution, long-slit mode with a 0.″8 slit and the R500B grism. In this configuration, the resolution is $R \sim 540$, and we have 3.54 Å pix^{-1} from ~3700 to 7200 Å. The slit was oriented along the line of the arc structure of the lensed source (PA of 64.°22). We grouped observations in two observing blocks of two exposures of 1385 s each with a 60 s acquisition image per block in the g band (see Figure 2). The seeing limited image shows an arc-like galaxy in the expected position for which we measured $g_{\rm AB} = 22.85 \pm 0.03$ for region 1 and $g_{\rm AB} = 23.43 \pm 0.04$ for region 2. The spectroscopic observations, with a total integration time of 5540 s, were reduced using the noao/twodspec and noao/onedspec packages of IRAF to yield fluxed, wavelength-calibrated spectra. We extracted spectra for the full arc region along the slit and separately for encircled regions 1 and 2. Our GTC spectroscopy reveals that the two regions in the arc are the same source. In Figure 3, we show the individual spectra for each arc region and the total arc spectrum. The spectra of the two arc regions show strong absorption features. We derive the redshift from the fit of well-measured lines of Si II λ1260.4, OI λ1302, C II λ1334.5, Si II λ1526.7, and Al II λ1670.7; for the full arc we find $z = 2.0448 \pm 0.0004$.

3.2. Gemini Spectroscopy

Archival GEMINI NIR-spectroscopic observations were found in CADC for region 1 of the arc. The spectrum was obtained using the cross-dispersed (XD) mode of the Gemini Near-IR Spectrograph on the 8.1 m Gemini-North telescope on the night of 2014 May 10 (under PI: Jane Rigby program ID: XGN-2014A-C-3) with the "short blue" camera, 32 l/mm grating and 0.″68 slit. The slit used in this XD mode is 7″ in length and the orientation was with a position angle (PA) of 89.°7 in region 1. The telescope was nodded (typically 3.″5 distant) in an ABBA-type pattern. We took the raw and calibration data from the CADC and reduced them using the Gemini IRAF package version v1.13.1 and following Mason et al. (2015) and the instruction on the Reducing XD spectra

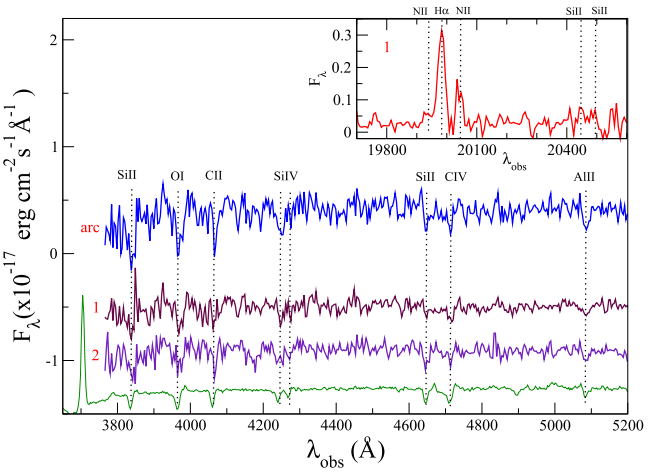

Figure 3. GTC/OSIRIS spectra of the two regions (up) and for the each individual regions (both downshifted for clarity). We mark the positions of the absorption features identified in the spectra. For comparison, we show the composite spectrum of LBGs from Shapley et al. (2003). We also show in the inset the Gemini spectrum for region 1 and mark the emission lines we identify; the H_α emission line yields a redshift for the source of $z = 2.0439$.

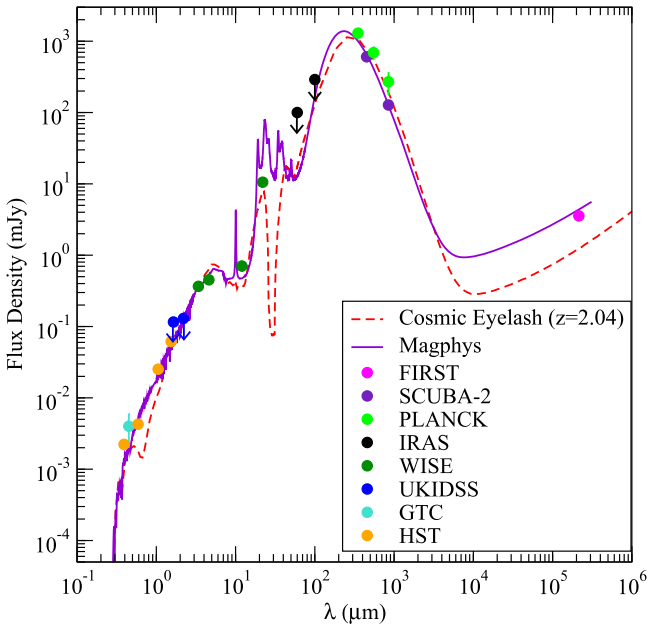

Figure 4. Multi-wavelength spectral energy distribution of the Cosmic Eyebrow. The SED of the Cosmic Eyelash shifted to $z = 2.044$ is consistent with the measurements of the galaxy at all frequencies from the optical to the radio.

webpage from GEMINI observatory.[11] The total integration time for the spectrum was 3600 s, and two telluric stars of spectral type A0V were observed immediately before and after the galaxy. Only in the K band have we found useful data with a clear detection of H_α in emission. In the inset of Figure 3, we show the spectrum near the H_α emission line from which we obtain a redshift of $z = 2.0439 \pm 0.0006$ in agreement with the rest-frame UV-spectrum. This redshift is consistent with the value published in Oguri et al. (2012; $z \approx 2.04$) for a source coincident in position with the lensed galaxy.

4. Analysis and Discussion

4.1. Lens Modeling

We have used Lenstool[12] (Kneib et al. 1993; Jullo et al. 2007) to perform a mass reconstruction of the foreground cluster, assuming a parametric model for the distribution of dark matter. This model was constrained using the location of the multiple images identified in the cluster. We used a simple model with a single cluster-scale mass component, as well as individual galaxy-scale mass components centered on each cluster member. For each component, we used a dual pseudo-isothermal elliptical mass distribution (dPIE, also known as a truncated PIEMD; Limousin et al. 2005). Sextractor and visual inspection of the *HST/WFPC3* images provided an identification of six families of multiply lensed background galaxies, arclets with two to six components each, based on proximity, colors, and shape. The redshift of the family of the Cosmic Eyebrow (A in Figure 1) was fixed at $z = 2.044$, and for the other families was set as a free parameter. When modeling the lensing, the redshift of three families (B, C, and E in Figure 1) was found very close to $z = 2.044$, so we fixed it to $z = 2.044$ and for only two families were the redshifts considered a free parameter. We checked the model with the reconstruction of the arclets, and found good agreement between the positions for image arcs and the reconstruction of each component of the families. The data are best fitted with a cluster-scale potential of ellipticity $e = 0.226$, PA $= 47\overset{\circ}{.}00$, and velocity dispersion $\sigma_{\rm PIEMD} = 830\,{\rm km\,s^{-1}}$. The enclosed mass within an aperture of 250 kpc is $M = 1.8 \pm 0.5 \times 10^{14}\,M_\odot$ with an Einstein radius of $\theta_{\rm e} = 11. \pm 0\overset{''}{.}4$ at $z = 2.044$. The amplification is obtained from the comparison between the main characteristic of the galaxies in the source plane and in the image plane; we find an amplification factor of 11 ± 2 for the two main members of the Cosmic Eyebrow family, which are our spectroscopy regions on the arc indicated in Figure 2. The mean amplification factors for each family with $z = 2.044$ are $A \sim 11 \pm 2$, $B \sim 7 \pm 2$, $C \sim 14 \pm 2$, and $E \sim 7 \pm 2$. The largest amplification is for the brightest member of family $C \sim 20 \pm 2$; for the other two families the mean amplification factors are $D \sim 4 \pm 2$ ($z \sim 2.9$) and $F \sim 5 \pm 2$ ($z \sim 1.0$).

4.2. SED

We plot the SED (Figure 4) assuming the lensed source in the *HST* and GTC images is the counterpart of the SCUBA-2 and *WISE* detections (all positions coincident within 1 arcsec) and list the photometry data in Table 1. We calculate the upper limit for the K_s and H bands from the UKIDSS catalog[13] and for 60 and 100 μm from the *IRAS* Sky Survey Atlas.[14] This SED is consistent with a source at redshift $z = 2 - 2.5$, and as expected, it is very well fitted by the SED of the Cosmic Eyelash in that redshift range. At all frequencies from optical to radio, the Cosmic Eyebrow is brighter than the Cosmic Eyelash.

We calculate the rest-frame 8–1000 μm luminosity, $L_{\rm IR}$, from direct integration of the data fit, and obtain an intrinsic luminosity for our galaxy $L({\rm Eyebrow}) = (1.3 \pm 0.1) \times 10^{13}\,L_\odot$, indicating an SFR of $\sim$2000 $M_\odot\ {\rm yr}^{-1}$ (Kennicutt 1998), which assumes

[11] http://www.gemini.edu/sciops/instruments/gnirs
[12] https://projets.lam.fr/projects/lenstool/wiki
[13] http://wsa.roe.ac.uk/
[14] http://irsa.ipac.caltech.edu/applications/IRAS/ISSA/

Table 1
Photometry

Wavelength(μm)	Flux (mJy)[a,b]	Observatory/Instrument
0.3921	0.0022 ± 0.0001	*HST/WFC3*
0.45	0.004 ± 0.002	GTC/OSIRIS
0.5887	0.0043 ± 0.0001	*HST/WFC3*
1.0552	0.0252 ± 0.0004	*HST/WFC3*
1.5369	0.0614 ± 0.0006	*HST/WFC3*
1.644	<0.112[c]	UKIDSS
2.199	<0.110[c]	UKIDSS
3.4	0.37 ± 0.01	*WISE*
4.6	0.45 ± 0.02	*WISE*
12	0.7 ± 0.1	*WISE*
22	10.6 ± 0.8	*WISE*
60	<100[c]	*IRAS*
100	<300[c]	*IRAS*
450	604 ± 86	SCUBA-2
850	127 ± 11	SCUBA-2
350	1298 ± 200	*Planck*
550	692 ± 100	*Planck*
850	271 ± 90	*Planck*
21.4[d]	3.56 ± 0.14	FIRST

Notes.
[a] Uncorrected for lensing amplification.
[b] Total arc flux.
[c] Flux upper limit.
[d] Wavelength in cm.

a Salpeter IMF, assuming a Chabrier IMF would possibly be a factor of ∼1.8 lower (Casey et al. 2014).

We also use the MAGPHYS code that allows us to fit simultaneously the ultraviolet-to-radio SED, so we can constrain physical parameters (Da Cunha et al. 2015). The fit is shown in Figure 4; we would benefit from measurements in photometric bands between 22 and 350 μm in order to establish which SED better describes the Cosmic Eyebrow. From this fit we give the median-likelihood estimates (and confidence ranges) of several physical parameters corrected for lensing amplification, stellar mass $\log(M_*/M_\odot) = 11.49^{+0.06}_{-0.05}$, star formation rate $\log(\mathrm{SFR}/M_\odot\ \mathrm{yr}^{-1}) = 2.73^{+0.02}_{-0.01}$, mass-weighted age $\log(\mathrm{age}_M\ \mathrm{yr}^{-1}) = 9.28^{+0.01}_{-0.01}$, average V-band dust attenuation $A_V = 3.30^{+0.02}_{-0.02}$, H-band mass-to-light ratio $\log(M_*/L_H) = 0.14^{+0.01}_{-0.01}$, total dust luminosity $\log(L_{\mathrm{dust}}/L_\odot) = 13.27^{+0.01}_{-0.02}$, luminosity-averaged dust temperature $T_{\mathrm{dust}}/K = 40^{+7}_{-2}$, and total dust mass $\log(M_{\mathrm{dust}}/M_\odot) = 9.19^{+0.15}_{-0.08}$. These physical parameters compare well with the average properties of the ALESS SMGs in Da Cunha et al. (2015). The SFR obtained with MAGPHYS is lower than estimated with the Kennicutt (1998) relation. This is partially due to the use of the Chabrier IMF and to the additional dust heating caused by the relatively old stellar populations of our galaxy that increases the dust luminosity at fixed SFRs (Da Cunha et al. 2015).

4.3. Spectroscopy

The UV rest-frame spectrum of the Cosmic Eyebrow resembles that of Lyman break galaxies (LBGs; Shapley et al. 2003) and displays the strong interstellar absorption features typical of the spectra of starburst galaxies (Casey et al. 2013). We identify in the observed spectrum low-ionization resonance interstellar metal lines such as Si II λ1260.4, OI 1302 Si II λ1304, C II λ1334, Si II λ1526, and Al II λ1670 that are associated with the neutral interstellar medium. We also detect high-ionization metal lines of Si IV $\lambda\lambda$1393, 1402 and C IV $\lambda\lambda$1548, 1550 that are associated with ionized interstellar gas and PCygni stellar wind features. The C IV feature exhibits a strong interstellar absorption component plus a weaker blue-shifted broad absorption and marginal evidence of redshifted emission associated with stellar winds that likely originate in main-sequence, giant, and supergiant O stars (Walborn & Panek 1984). Our data do not show evidence for the He II λ1640, which could be an indication of a low ratio of Wolf–Rayet to O stars (Schaerer & Vacca 1998).

In the spectrum of the region 1 of the arc, we find H_α at 19982 ± 4 Å and the [N II] λ6583 at 20041 ± 5 Å. Full width at half maximum (FWHM) line widths are 386 ± 20 km s^{-1} and 331 ± 20 km s^{-1}; after correction for the instrumental profile, we estimate that the intrinsic width of these lines is 150 ± 25 km s^{-1}. The low [N II]λ6583/H_α ratio of 0.33 ± 0.04 suggests a star-forming region (Kewley et al. 2013). The $\mathrm{EW}_{\mathrm{rest}}$ (H_α) = 111 ± 10 Å compares well with values reported in other well-known SMGs of a similar luminosity (Olivares et al. 2016).

5. Conclusions

A cross-match of the *AllWISE* and *Planck* compact source catalogs aimed to identify the brightest examples of SMGs in the full-sky uncovered *WISE* J132934.18+224327.3, the Cosmic Eyebrow, a $z = 2.0439 \pm 0.0006$ galaxy with a spectral energy distribution from mid-IR to submillimeter similar to that of the Cosmic Eyelash and higher observed fluxes. Archival data of SCUBA-2 and *HST* reveal a multiple lensed galaxy at the position of the strong submillimeter source. Follow-up observations with GTC/OSIRIS provided a precise redshift determination of the lensed galaxy and a rest-frame UV-spectrum with clearly identified low-ionization resonance interstellar metal lines that is consistent with that of starburst galaxies. Near-IR spectroscopy with Gemini-North showed H_α in emission at a strength consistent with values reported for other SMGs. This galaxy is gravitationally magnified by a massive cluster at $z = 0.44$; modeling with Lenstool indicates a lensing amplification factor of 11 ± 2. The intrinsic rest-frame 8–1000 μm luminosity of the lensed galaxy is (1.3 ± 0.1) × $10^{13}\,L_\odot$ indicating a likely SFR of ∼500–2000 $M_\odot\,\mathrm{yr}^{-1}$. The SED of this new SMG resembles the Cosmic Eyelash from optical/mid-IR to submillimeter/radio, albeit at higher intrinsic luminosity. It is one of the brightest examples of SMGs so far reported, which may enable detailed high spatial resolution studies of star-forming regions in such dusty galaxies.

Based on observations made with the GTC telescope, in the Spanish Observatorio del Roque de los Muchachos of the Instituto de Astrofísica de Canarias. This work has been partially funded by projects ESP2015-69020-C2-1-R, ESP2014-56869-C2-2-P, and AYA2015-69350-C3-3-P (MINECO). H.D. acknowledges financial support from the Spanish Ministry of Economy and Competitiveness (MINECO) under the 2014 Ramón y Cajal program MINECO RYC-2014-15686. We thank David Valls-Gabaud for his suggestions and comments on various aspects of this work. We are grateful to the anonymous referee for useful comments on the Letter.

References

Bayliss, M. B., Johnson, T., Gladders, M. D., Sharon, K., & Ogur, M. 2014, ApJ, 783, 41
Cañameras, R., Nesvadba, N. P. H., Guery, D., et al. 2015, A&A, 581, 105
Casey, C. M., Chen, C., Cowie, L. L., et al. 2013, MNRAS, 436, 1919
Casey, C. M., Narayanan, D., & Cooray, A. 2014, PhR, 541, 45
Chapman, S. C., Blain, A. W., Smail, I., & Ivison, R. J. 2005, ApJ, 622, 722
Da Cunha, E., Walter, F., Smail, I. R., et al. 2015, ApJ, 806, 110
Danielson, A. L. R., Swinbank, A. M., Smail, I., et al. 2011, MNRAS, 410, 1687
Hainline, L., Blain, A. W., Smail, I., et al. 2011, ApJ, 740, 96
Harrington, K. C., Yun, M. S., Cybulski, R., et al. 2016, MNRAS, 458, 4383
Hodge, J. A., Swinbank, A. M., Simpson, J. M., et al. 2016, ApJ, 833, 103
Iglesias-Groth, S., Díaz-Sánchez, A., Rebolo, R., & Dannerbauer, H. 2017, MNRAS, 467, 330
Ivison, R. J., Swinbank, A. M., Smail, I., et al. 2013, ApJ, 772, 137
Ivison, R. J., Swinbank, A. M., Swinyard, B., et al. 2010, A&A, 518, L35
Jones, S. F. 2015, PhD thesis, Univ. Leicester, https://core.ac.uk/download/pdf/42018134.pdf
Jullo, E., Kneib, J.-P., Limousin, M., Eliasdottir, A., Marshall, P. J., & Verdugo, T. 2007, NJPh, 9, 447
Kennicutt, R. C., Jr. 1998, ApJ, 498, 541
Kewley, L. J., Dopita, M. A., Leitherer, C., et al. 2013, ApJ, 774, 100
Kneib, J. P., Mellier, Y., Fort, B., & Mathez, G. 1993, A&A, 273, 367
Limousin, M., Kneib, J. P., & Natarajan, P. 2005, MNRAS, 356, 309
Mason, R. E., Rodríguez-Ardila, A., Martins, L., et al. 2015, ApJS, 217, 13
Michalowski, M., Hjorth, J. D., & Watsonet, D. 2010, A&A, 514, A67
Negrello, M., Hopwood, R., De Zotti, G., et al. 2010, Sci, 330, 800
Oguri, M., Bayliss, M. B., & Dahle, H. 2012, MNRAS, 420, 3213
Olivares, V., Treister, E., Privon, G. C., et al. 2016, ApJ, 827, 570
Planck Collaboration XVI, 2014, A&A, 571, A16
Schaerer, D., & Vacca, W. D. 1998, ApJ, 497, 618
Shapley, A. E., Steidel, C. C., Pettini, M. A., & Kurt, L. 2003, ApJ, 588, 65S
Simpson, J. M., Swinbank, A. M., Smail, I., et al. 2014, ApJ, 788, 125
Smail, I., Ivison, R. J., & Blain, A. W. 1997, ApJL, 490, 5
Smail, I., Ivison, R. J., Blain, A. W., & Kneib, J.-P. 2002, MNRAS, 331, 495
Strandet, M. L., Weiss, A., Vieira, J. D., et al. 2016, ApJ, 822, 80
Swinbank, A. M., Dye, S., Nightingale, J. W., et al. 2015, ApJL, 806, 17
Swinbank, A. M., Simpson, J. M., Smail, I., et al. 2014, MNRAS, 438, 1267
Swinbank, A. M., Smail, I., Longmore, S., et al. 2010, Natur, 464, 733
Vieira, J. D., Marrone, D. P., Chapman, S. C., et al. 2013, Natur, 495, 344
Vlahakis, C., Hunter, T. R., Hodge, J. A., et al. 2015, ApJL, 808, 4
Walborn, N. R., & Panek, R. J. 1984, ApJ, 280, 27
Weiß, A., De Breuck, C., Marrone, D. P., et al. 2013, ApJ, 767, 88